Investigation of the interaction between amodiaquine and human serum albumin by fluorescence spectroscopy and molecular modeling

ARTICLE *in* EUROPEAN JOURNAL OF MEDICINAL CHEMISTRY · MAY 2012

Impact Factor: 3.45 · DOI: 10.1016/j.ejmech.2012.05.007 · Source: PubMed

5 AUTHORS, INCLUDING:

Bahram Hemmateenejad
Shiraz University
183 PUBLICATIONS **2,723** CITATIONS
SEE PROFILE

Taghi Khayamian
Isfahan University of Technology
107 PUBLICATIONS **1,562** CITATIONS
SEE PROFILE

Sajjad Gharaghani
University of Tehran
11 PUBLICATIONS **122** CITATIONS
SEE PROFILE

European Journal of Medicinal Chemistry 54 (2012) 255–263

Contents lists available at SciVerse ScienceDirect

European Journal of Medicinal Chemistry

journal homepage: http://www.elsevier.com/locate/ejmech

Original article

Investigation of the interaction between amodiaquine and human serum albumin by fluorescence spectroscopy and molecular modeling

Fayezeh Samari [a], Mojtaba Shamsipur [b], Bahram Hemmateenejad [a,*], Taghi Khayamian [c], Sajjad Gharaghani [c]

[a] Department of Chemistry, Shiraz University, Department of Chemistry, Adabiat Four-way, Shiraz, Fars 71454, Iran
[b] Department of Chemistry, Razi University, Kermanshah, Iran
[c] School of Chemistry, Isfahan University, of Technology, Isfahanm, Iran

HIGHLIGHTS

- The interaction between amodiaquine and human serum albumin has been investigated.
- The results obtained revealed that amodiaquine has moderate affinities for HAS and binds mainly to sub-domain IIA.
- Hydrogen bonding formation and van der Waals forces play major role in the binding process.
- The binding study was also modeled by molecular docking and molecular dynamic simulation.

GRAPHICAL ABSTRACT

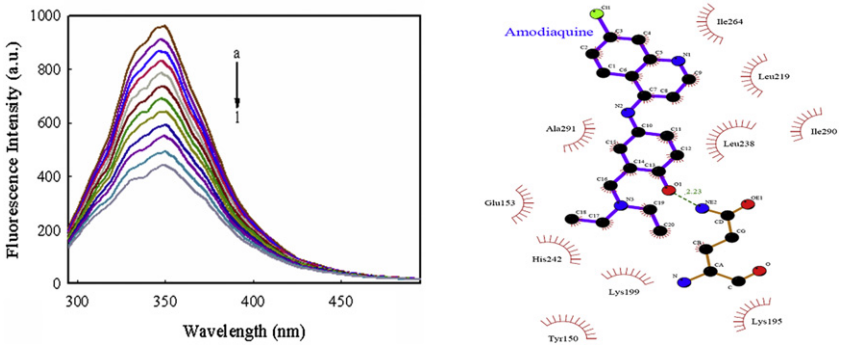

ARTICLE INFO

Article history:
Received 9 March 2012
Received in revised form
28 April 2012
Accepted 3 May 2012
Available online 12 May 2012

Keywords:
Human serum albumin
Amodiaquin
Fluorescence
Binding
Molecular modeling

ABSTRACT

The interaction of amodiaquine (AQ) with human serum albumin (HSA) has been studied by fluorescence spectroscopy. Based on the sign and magnitude of the enthalpy and entropy changes ($\Delta H^0 = -43.27$ kJ mol^{-1} and $\Delta S^0 = -50.03$ J mol^{-1} K^{-1}), hydrogen bond and van der Waals forces were suggested as the main interacting forces. Moreover, the efficiency of energy transfer and distance between HSA and acceptor AQ was calculated. Finally, the binding of AQ to HSA was modeled by molecular docking and molecular dynamic simulation methods. Excellent agreement was found between the experimental and theoretical results. Both experimental results and modeling methods suggested that AQ binds mainly to the sub-domain IIA of HSA.

1. Introduction

Malaria is still one of the major burdens of public health in sub-Saharan Africa. According to the last world health organization report, in the year 2010, 106 countries and areas are considered to be endemic for malaria with 750 million people at risk of contracting the disease; 225 million cases of malaria in 2009 was indicate that led to nearly a 781,000 deaths, mostly among African children under 5 years [1]. Amodiaquine (AQ, Fig. 1), for its chemical structure, is an established antimalarial drug recently reintroduced in the World Health Organisation Model List of Essential Medicines [2]. AQ is a 4-

* Corresponding author. Tel.: +98 711 613 7360; fax: +98 711 228 6008.
E-mail address: hemmatb@sums.ac.ir (B. Hemmateenejad).

0223-5234/$ – see front matter © 2012 Elsevier Masson SAS. All rights reserved.
doi:10.1016/j.ejmech.2012.05.007

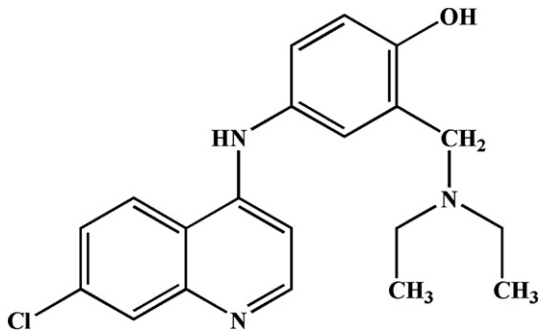

Fig. 1. The chemical structure of amodiaquine.

aminoquinoline similar to chloroquine in structure and activity, has been used as an antimalarial, an antipyretic and an anti-inflammatory agent [3]. Despite cross-resistance between chloroquine and AQ, AQ is more effective than chloroquine in areas with identified chloroquine-resistance. Therefore AQ was chosen by several countries as the first-line drug in combination with artesunate [4].

Serum albumin (SA), as the most abundant protein in blood plasma, functions as a shuttle for various endogenous and exogenous ligands such as fatty acids, hormones, and foreign molecules including drugs [5]. Therefore, SA plays an important role in the distribution, free concentration, excretion, metabolism and interaction with the target tissues of these ligands [6]. The nature and magnitude of drug–protein interaction significantly influences the biological activity of the drug. Weak binding leads to a short lifetime or poor distribution of ligands, whereas strong binding decreases the concentrations of free ligands in plasma [7]. Consequently, investigations on the affinity and the interaction mechanisms of ligands to serum albumins, which may provide some useful information about therapeutic effective of drugs in pharmacology and pharmacodynamics and design of dosage forms, are of fundamental importance [8]. Moreover, an understanding of the chemistry of the various classes of pharmaceutical interactions with albumin can suggest new approaches to design and drug therapy [9]. For these reasons, in recent years, the interactions of many drugs with SA were studied [10–15].

Human serum albumin (HSA) is a widely studied protein for over 40 years due to its ability to extraordinary binding capacity, availability, stability and altered pharmacokinetic properties [16]; it is also because its primary structure is well-known for a long time and its tertiary structure has been determined by X–ray crystallography. Structurally, HSA is a nonglycosylated consisting of a single peptide chain of 585 amino acids, largely helical (~67%), with the remaining polypeptide occurring in turns and extended or flexible regions between sub-domains with no β-sheets and having 67 kDa mass, organizes to form a heart shaped protein [5]. HSA consists of three homologous domains, namely, I (residues 1–195), II (196–383), and III (384–585), each domain being divided into sub-domains A and B, and the overall structure is stabilized by 17 disulfide bridges [5]. The specific physiological activity of the aromatic and heterocyclic ligands upon complexation with serum albumin originates from the presence of two hydrophobic pockets in sub-domains IIA (site I) and IIIA (site II) [17]. HSA contains a single intrinsic tryptophan residue at position 214 in domain IIA, where a large hydrophobic cavity is present, and its fluorescence is sensitive to the ligands bonded nearby [18]. Therefore, information about the HSA can be obtained by the measurement of intrinsic fluorescence intensity of the tryptophan residue before and after addition of the drug.

To the best of our knowledge, there is only one report on the interaction between AQ and HSA, in which the authors studied the interaction of 5 antimalarial drugs with HSA α1-acid glycoprotein (AAG) [19]. For interaction of AQ with HSA only association constant has been reported by circular dichroism spectroscopy and affinity chromatography. No detailed study on the interaction of AQ and HSA by spectophotometry and computational methods has been reported. In the present work, we have employed a combination of experimental and computational approaches, in an attempt to determine where and how AQ, as the most common antimalarial drug, bind to HSA under physiological conditions. In order to determine the affinity of AQ to HSA and investigate the thermodynamics of their interaction, we carried out investigations on HSA–AQ association using fluorescence spectroscopy at different temperatures. The site marker competitive experiments were also carried out to determine the specific binding site of AQ to HSA. Along with synchronous fluorescence spectra, we planned to further investigate the conformational change of HSA in buffer solution. In addition, the distance between HSA as donor and AQ as acceptor was also evaluated by means of the Förster energy transfer theory. Meanwhile, the binding of AQ to HSA was investigated by docking and molecular dynamic (MD) simulations methods. The results of experimental and theoretical studied were compared and comments were given on the mechanism of binding. This study may provide valuable information related the biological effects of AQ and therapeutic effect of this drug in pharmacology and pharmacodynamics.

2. Experimental section

2.1. Materials

Human serum albumin (fatty acid–free HSA), amodiaquine hydrochloride, warfarin and ibuprofen were purchased from Sigma Aldrich (St. Louis, MO, USA) and used without further purification. A stock solution of HSA was prepared by dissolving proper amount of solid HSA in a 0.05 M Tris–HCl buffer of pH 7.4 containing 0.1 M sodium chloride (to maintain the ionic strength of solution) and was kept in the dark at refrigerator for about a week only. A 1.1×10^{-6} M working solution of HSA at pH 7.4 was prepared by appropriate dilution of the stock solution. A 1.0×10^{-3} M stock solution of AQ was prepared by dissolving an appropriate amount of the drug in doubly distilled water. Stock solutions of warfarin and ibuprofen (1.0×10^{-3} M) were prepared by dissolving appropriate amount of the drugs in DMSO. All other chemicals were of analytical grade and used without further purification. Doubly distilled water was used throughout.

2.2. Apparatus

All fluorescence spectra were recoreded on a LS–55 Spectrofluorometer (Perkin–Elmer Co., USA) equipped with a water bath and a quartz cell (10–mm). The FL WinLab Software (Perkin–Elmer) was used to digitize the measured data.

UV–vis absorption spectra were recorded on a Shimadzu UV–1650PC UV–vis spectrophotometer (Japan) with a 10–mm quartz cuvette at room temperature.

The pH values were potentiometrically measured using a Metrohm 654 pH–meter equipped with a combined glass electrode (pH Electrode Blue Line 23 pH, Schott).

2.3. Spectroflourimetric experiments

2.3.1. Binding assay

In each assay, 3.0 mL portion of HSA solution with a concentration of 1.1×10^{-6} M was added accurately into the quartz cell and it was titrated by successive additions of a 1.0×10^{-3} M stock solution

of AQ by a micro syringe in time intervals of 10 min. The fluorescence emission spectra were recorded over a wavelength region of 295–500 nm (λ_{ex} of 280 nm) at temperatures of 291, 301 and 310 K. It should be noted that, in the course of increasing concentrations of the AQ, an instrumental inner filter effect (IFE) caused some decrease in the fluorescence emission intensity. This effect is an inherent problem of many fluorimetric procedures which lead to the results depart from the initial linearity [20] and must therefore be taken into account. Thus, the fluorescence intensities were corrected for absorption of exciting light and reabsorption of the emitted light to decrease the inner filter effect according to the following relationship [21]:

$$F_{cor} = F_{obs}\exp[(A_{ex} + A_{em})/2] \quad (1)$$

where F_{cor} and F_{obs} are corrected and observed fluorescence intensities, respectively, and A_{ex} and A_{em} are the absorption of the AQ at the excitation and the emission wavelengths, respectively. The intensity of fluorescence used in this paper is the corrected fluorescence intensity.

The width of the excitation and emission slits was set at 10.0 and 5.0 nm, respectively, while the scanning rate was 1000 nm min^{-1}. Synchronous fluorescence spectra were collected in the synchronous scan mode with an offset of 15 or 60 nm ($\Delta\lambda = \lambda_{em} - \lambda_{ex} = 15$ or 60 nm). Each spectrum was the average of three successive scans.

2.3.2. Site marker competitive experiments

Binding location studies between AQ and HSA in the presence of two site markers, namely warfarin and ibuprofen, were measured using a fluorescence titration method. The concentrations of HSA and site markers were set at equimolar concentration (1.1×10^{-6} M). Before displacement, ibuprofen or warfarin was incubated with HSA in a Tris–HCl buffer solution for 30 min. Then, 3.0 mL sample was added into a 1.0 cm quartz cuvette, followed by titration of aliquots of AQ at 291 K. The emission intensity of mixture was then monitored and recorded from 295 to 500 nm at a λ_{ex} of 280 nm; for warfarin solution alone, the fluorescence data were collected from 330 to 500 nm at a λ_{ex} of 320 nm.

2.4. Molecular modeling and docking

The molecular docking Arguslab 4.0.1 program was employed to generate a docked conformation of AQ with HSA [22]. LIGPLOT [23], a program for automatically plotting protein–ligand interactions, was used to analyze the interactions between HSA and AQ.

2.4.1. Chemical structures of protein and ligand

The chemical structure of the AQ was constructed by Hyperchem package (Ver. 7.0), and energy minimization for AQ was performed by AM1 semi empirical method with Polak–Ribiere algorithm until the root mean square gradient of 0.01 kcal mol^{-1}. The known crystal structure of HSA (PDB Id: 1AO6) was obtained from the Brookhaven Protein Data Bank. Water molecules were removed, and hydrogen atoms were added. An Arguslab was applied to find out the best conformation of the AQ with HSA.

2.4.2. Molecular dynamics simulations

The MD simulations were performed using the GROMACS (GROningen Machine for Chemical Simulations) 4.5.1 package [24,25]. The topology parameters of HSA were created by using the Gromacs program. The interaction parameters were computed using the GROMOS96 43a1 force field [26], with the intermolecular (nonbonded) potential represented as a sum of Lennard-Jones (LJ) force and pair-wise Coulomb interaction; the long-range electrostatic interactions were calculated by the particle-mesh Ewald (PME) method [27]. The velocity Verlet algorithm was used for the numerical integrations [28], and the initial atomic velocities were generated with a Maxwellian distribution at a given absolute temperature [29]. The coordinate of AQ was transferred into Gromacs topologies using the PRODRG2.5 server (beta) [30]. Then the complex was immersed in a cubic box ($11.37 \times 11.37 \times 11.37$ nm^3) of extended simple point charge (SPC) water molecules [31]. The solvated system was neutralized by adding sodium ions in the simulation, and the entire system was composed of 5843 atoms of HSA, one AQ, 15 Na^+ counter ions and 43,616 solvent atoms.

The energy was minimized using the steepest descent method of 1000 steps with a cutoff of 9 Å for van der Waals and Coulomb forces. Simulations were performed using an NPT (constant number of molecules, constant pressure, and constant temperature) ensemble [32] using the Berendsen thermostat [33] with coupled temperature and pressure of 300 K and 1 bar, respectively. In the first stage of equilibration, the solutes (protein, counter ions and AQ) were fixed and the position-restrained dynamics simulation of the system, in which the atom positions of HSA were restrained at 300 K for 20 ps. Finally, the full system was subjected to 6000 ps MD at 300 K temperature and 1 bar pressure. The periodic boundary condition was used and the motion equations were integrated by applying the leap–frog algorithm with a time step of 2 fs. The atom coordinates were recorded every 1 ps during the simulation for latter analysis. The MD simulation and results analysis were performed on the open SUSE 11.3 Linux on an Intel Core 2 Quad Q6600 2.4 GHz and 4 GB of RAM.

3. Results and discussion

3.1. Fluorescence quenching measurements

The fluorescence emission spectra of HSA in the presence of different added amounts of AQ are shown in Fig. 2A. It is observed a gradual decrease in the initial HSA fluorescence emission, without notable changes in the wavelength of maximum emission. Decreasing in fluorescence intensity of fluorophore (called as quenching) can be induced by a variety of molecular interactions [21]. The mechanisms of quenching are usually classified as either dynamic (collisional encountering between the fluorophore and quencher) or static (formation of a non-fluorescent ground state complex) [21].

In our analysis, the fluorescence quenching was treated by Stern–Volmer equation, as:

$$F_0/F = 1 + K_{sv}[Q] = 1 + k_q\tau_0[Q] \quad (2)$$

where F_0 and F are the fluorescence intensities in the absence and presence of the quencher, respectively, K_{sv} is the Stern–Volmer quenching constant, [Q] is the concentration of the quencher, τ_0 is the average lifetime of molecule without quencher and k_q is quenching rate constant of bimolecule. The possible quenching mechanism can be interpreted by following the changes in K_{sv} as function of temperature [21]. The Stern–Volmer plots for quenching of the fluorescence emission of HSA by AQ at three temperatures (i.e., 291, 301 and 310 K) are shown in Fig. 2B and the estimated parameters of Eq. (2) are listed in Table 1. The results reveal that the Stern–Volmer quenching constant K_{sv} is inversely correlated with temperature, which confirms that the probable quenching mechanism of fluorescence of HSA by AQ is not initiated by dynamic collision, instead it is came from compound formation. The value of k_q also gives information about the mechanism of quenching. It is well-known that the maximum scatter collision quenching constant k_q of various quenchers with a biopolymer is 1.0×10^{10} L mol^{-1} s^{-1} [21]. To calculate k_q, we need the value of τ_0, which for biomacromolecule it is assumed to be 10^{-8} s [34]. As it is obvious from Table 1, the quenching constants of HSA by AQ,

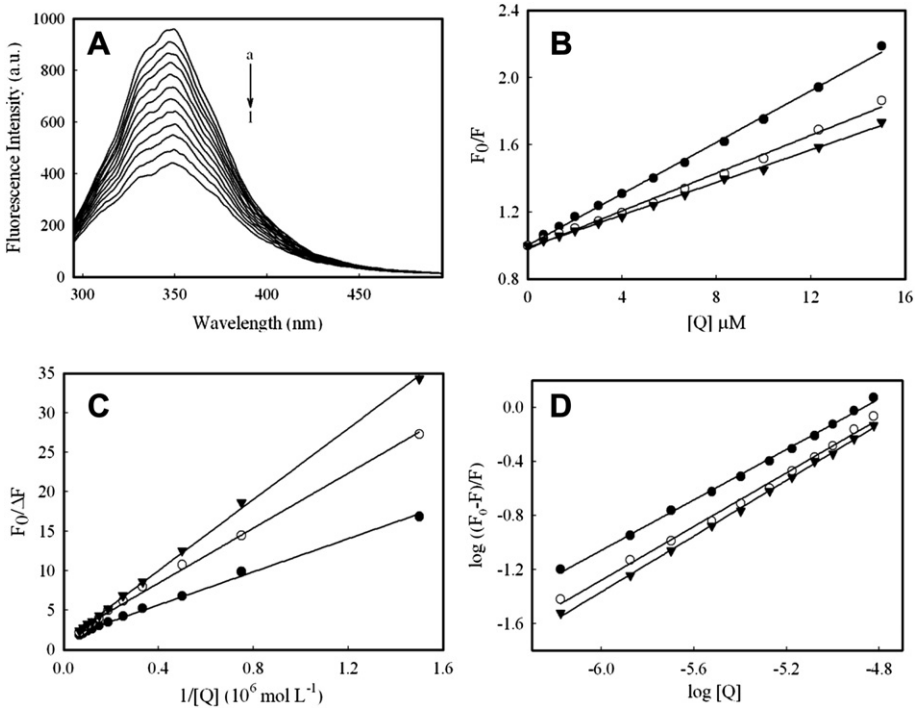

Fig. 2. (A)Fluorescence spectra of HSA with AQ at 291 K. The concentrations of HSA was 1.1×10^{-6} M; AQ: (a) 0.0, (b) 0.7, (c) 1.3, (d) 2.0, (e) 3.0, (f) 4.0, (g) 5.3, (h) 6.7, (i) 8.3, (j) 10.0, (k) 12.3, (l) 15.0×10^{-6} M. (B) Stern–Volmer plot for quenching HSA with AQ in buffer solution (C) The modified Stern–Volmer plots of HSA on the different temperature with AQ. $\lambda_{ex} = 280$ nm. (D) Double-log plots of AQ quenching effect on HSA fluorescence at 291 K (◆), 301 K (■) and 310 K (▲) pH 7.4 and λ_{ex}: 280 nm.

calculated at different temperatures, are larger than the suggested threshold value for scatter collision, which is another indication of the static quenching. Since the quenching mechanism is most probably proceeding by complex formation (static quenching), the quenching process was further analyzed according to the modified Stern–Volmer equation [21]:

$$\frac{F_0}{\Delta F} = \frac{F_0}{F_0 - F} = \frac{1}{f_a K_a}\frac{1}{[Q]} + \frac{1}{f_a} \tag{3}$$

where, ΔF is the difference in fluorescence intensity in the presence (F) of the quencher at concentration [Q] and in the absence of quencher (F_0). The parameter K_a is the effective quenching constant for the accessible fluorophores, which is analogous to the associative binding constants for the quencher-acceptor system [35], and f_a is the fraction of accessible fluorescence. As it is observed from Fig. 2C, the dependence of $F_0/\Delta F$ on the reciprocal value of the quencher concentration $[Q]^{-1}$ is linear at all studied temperatures. The estimated fitting parameters are shown in Table 2. The decreasing trend of K_a with increasing temperature is in accordance with K_{sv}'s dependence on temperature as mentioned above.

It should be noted that the above plots and data were obtained after correction of fluorescence intensity for reabsorption of the emitted fluorescent light by the quencher (sing Eq. (1)). To show the effect of the fluorescence correction on the binding data, the Stern–Volmer plots and the corresponding data were recalculated using non-corrected data. The results are given in the Supplementary materials. It is observed that the Stern–Volmer plots are linear; however in some instances the degree of linearity (as measured by R) is lower for non-corrected fluorescence data. In addition, the calculated K_{SV} data from the non-corrected data are significantly higher than those obtained from the corrected values. These observations confirm that correction for reabsorption of light is essential for our study and using of non-corrected data results in large error in estimation of the binding data.

3.2. Analysis of binding equilibria

When small molecules bind independently to a set of equivalent sites on a macromolecule, the equilibrium between free and bound molecules is given by the Eq. (4) [36]:

$$\log\frac{F_0 - F}{F} = \log K_b + n\log\left[Q\right] \tag{4}$$

where K_b and n are the apparent binding constant and the number of binding sites, respectively. Fig. 2D shows the corresponding double–logarithm curve and Table 3 gives the calculated results. As it is seen from Table 3, values of n are approximately equal to 1, which indicate the existence of just a single binding site in HSA for

Table 1
Stern–Volmer quenching constants (K_{SV}) and bimolecular quenching rate constant (k_q) of the interaction of AQ with HSA at different temperatures.

T (K)	10^{-4} K_{SV} (M^{-1})	10^{-12} k_q (M^{-1} s^{-1})	[a]R
291	7.663	7.663	0.998
301	5.621	5.621	0.994
310	4.840	4.840	0.998

[a] R is the linear correlated coefficient.

Table 2
Modified Stern–Volmer association constant K_a and relative thermodynamic parameters at pH 7.40.

T (K)	10^{-4} K_a(M^{-1})	[a]R	ΔH^0 (kJ mol^{-1})	ΔG^0 (kJ mol^{-1})	ΔS^0 (J mol^{-1} K^{-1})
291	13.80	0.996	−43.27	−28.71	−50.03
301	8.39	0.997		−28.21	
310	4.59	0.999		−27.76	

[a] R is the linear correlated coefficient.

Table 3
Binding parameters of the system of the interaction AQ with HSA at different temperatures.

T (K)	10^{-4} K_b (M^{-1})	n	[a]R
291	3.50	0.93	0.998
301	4.86	0.99	0.995
310	6.73	1.03	0.999

[a] *R* is the linear correlated coefficient.

AQ; the estimated values of K_b are in the order of 10^4, indicating that there is a moderately strong attraction between AQ and HSA. The obtained values are very close to the affinity value determined previously by affinity chromatography ($nK_a \approx 2 \times 10^4$) [19]. These results together with the estimated effective quenching constants suggest that the binding constant between AQ and HSA is moderate and hence AQ can be stored and carried by this protein in the body.

3.3. Thermodynamic parameters for binding of AQ to HSA

The interaction forces between a small molecule and a macromolecule include four types of interactions, namely hydrogen bonding, van der Waals interactions, electrostatic forces and hydrophobic interactions [37]. Since the temperature effect was very small in the studied range of temperature, the interaction enthalpy change can be regarded as a constant. Therefore, the enthalpy (ΔH^0) and entropy changes (ΔS^0) can be calculated using the van't Hoff equation:

$$\ln K = -\left(\frac{\Delta H^0}{RT}\right) + \left(\frac{\Delta S^0}{R}\right) \quad (5)$$

where K is analogous to the effective quenching constants K_a at the corresponding temperature [35] and R is the gas constant, ΔH^0 and ΔS^0 are the enthalpy and entropy changes, respectively. From the temperature dependence of the binding constants (Fig. 3), the thermodynamic functions involved in the binding process were calculated (Table 2). The negative sign for free energy (ΔG^0) means that the binding process is spontaneous. From Table 2, ΔH^0 and ΔS^0 for the binding interaction between AQ and HSA were calculated to be -43.3 kJ mol^{-1} and -50.0 J mol^{-1} K^{-1}, respectively. The negative values of ΔH^0 and ΔS^0 indicate that the binding is mainly enthalpy driven, whereas the entropy is unfavorable for it. According to Ross' view [38], the signs and magnitudes of thermodynamic parameters (ΔH^0 and ΔS^0) for protein reactions can account for the main forces contributing to protein stability. From the thermodynamic standpoint, $\Delta H^0 > 0$ and $\Delta S^0 > 0$ implies a hydrophobic interaction, $\Delta H^0 < 0$ and $\Delta S^0 < 0$ reflects the van der Waals force or hydrogen bond formation and $\Delta H^0 < 0$ and $\Delta S^0 > 0$ suggesting an electrostatic force. The negative ΔH^0 and ΔS^0 values of the interaction of AQ with HSA indicate that the binding process investigated here is mainly driven by van der Waals force and hydrogen bonding.

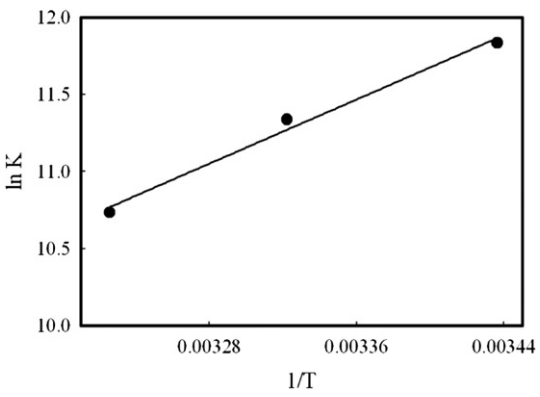

Fig. 3. Van't Hoff plot for the interaction of HSA and AQ in Tris buffer, pH 7.40.

3.4. Identification of binding site of AQ on HSA

To identify the binding site location of AQ on the region of HSA, the competitive experiment was carried out using two site markers. Warfarin, an anticoagulant drug, is a well-known marker of site I (hydrophobic sub-domain IIA) of HSA [39] and ibuprofen, a nonsteroidal anti-inflammatory agent, have been considered as stereotypical ligands for Sudlow's sites II (sub-domain IIIA) of HSA [35]. In the competitive experiments of site markers, AQ was gradually added to the solutions containing equimolar concentrations of HSA and each one of the site markers (1.1×10^{-6} M). Since the site markers have low solubility in water, the stock solutions of these compounds were prepared in DMSO. So, a question is that does DMSO alter protein conformation? Actually, DMSO as a small ligand may interact with HSA. However, Ojha et al. in their study [40] found that addition of DMSO to water (up to the concentration of 15% DMSO) induced no major structural changes in BSA, which is similar in structure to HSA. In our study, the amount of the added DMSO was very small, i.e., 3.3 μL of solutions of site markers were added to 3.0 mL (or 3000 μL) aqueous solution of HSA, where the final solution was containing about 0.1% of DMSO. So, it is unlikely that DMSO at the used level could alter the conformation of HSA. Using of DMSO for studying the interaction of site markers with HSA has been already reported in many studies, for examples see the Refs. [40–44].

The fluorescence spectra were recorded at 291 K with an excitation wavelength of 280 nm in the range of 295–500 nm. The results are shown in Fig. 4. Obviously, by addition of AQ to the solution of HSA–warfarin complex, the fluorescence intensity of the HSA decreased gradually in accompanying with a red shift in the maximum emission wavelength. This suggests an increase in the polarity of the region surrounding the tryptophan site (Trp214) [18], and indicating that the binding of AQ to HSA was affected by addition of warfarin. In addition, the red shift in the emission spectra can be attributed to the escaping of warfarin, which emits light at longer wavelengths than HSA, from the binding site of HSA. In contrast to warfarin, the fluorescence intensity of HSA in presence of ibuprofen (Fig. 4B) was almost the same as in the absence of ibuprofen (see Fig. 2A for comparison), indicating that ibuprofen did not prevent the usual binding location of AQ on HSA.

Fig. 4C shows the changes in the fluorescence spectra (with excitation wavelength of 320 nm, in which warfarin molecules are excited whereas HSA molecules do not) of warfarin–HSA complex in the presence of different added amounts of AQ. The weak fluorescence intensity of warfarin in the range of 330–500 nm could be enhanced on binding with HSA when warfarin excited at 320 nm (the maximum absorption wavelength of warfarin) [44]. As demonstrated in Fig. 4C, addition of AQ to HSA–warfarin mixture resulted in a decrease in the fluorescence intensity and a slight red shift of maximum emission wavelength from 381 to 385 nm. The red shift of λ_{max} suggested an increase in polarity around warfarin, a reasonable explanation was that some of the bound warfarin fell out of the binding site and exposed to water [45]. That was to say, binding of AQ led to a disruption of HSA–warfarin complex. Thus, it can be concluded that the binding site of AQ is located in drug site I with partial rather than complete overlap with warfarin binding site.

Moreover, to make sure about the binding site of AQ on HSA, the experiment data of Fig. 4A and B were analyzed using the modified Stern–Volmer and the quenching constants were calculated. The

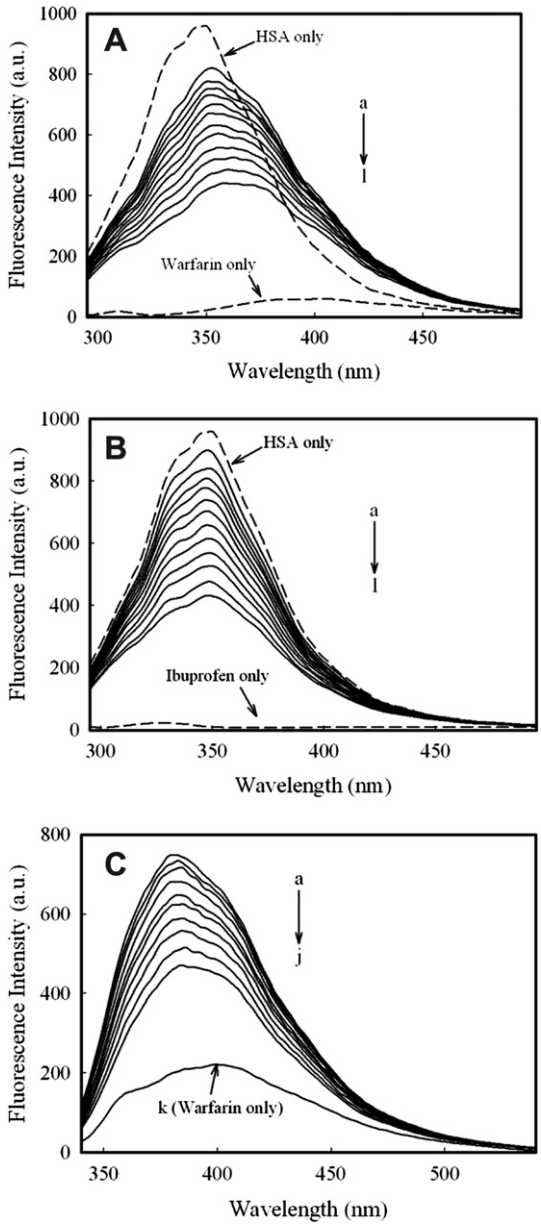

Fig. 4. Effect of site marker to the AQ–HSA system (T = 291 K). (A) $C_{Warfarin} = C_{HSA} = 1.1 \times 10^{-6}$ M (λ_{ex} = 280 nm); (B) $C_{Ibuprofen} = C_{HSA} = 1.1 \times 10^{-6}$ M (λ_{ex} = 280 nm); $C_{AQ} \times 10^{-6}$ M, a–l: 0.0, 0.7, 1.3, 2.0, 3.0, 4.0, 5.3, 6.7, 8.3, 10.0, 12.3, 15.0. (C) Titration of warfarin–HSA by AQ with concentrations from 0 to 1.5×10^{-5} M, (a) to (j); curve k shows the emission spectrum of warfarin only. $C_{HSA} = C_{Warfarin} = 1.1 \times 10^{-6}$ M, λ_{ex} = 320 nm.

results are given in Table 4. The results show that the binding constant was surprisingly lower in the presence of warfarin (about 47% reduction), while the constants of the system with and without ibuprofen had only a little difference (about 18% reduction), indicating that there was a significant competition between AQ and warfarin for HSA. Based on the experimental results and analysis mentioned above, we inferred that the binding site of AQ was mainly located within site I (sub-domain IIA) of HSA.

3.5. Investigation of HSA conformation changes

To explore the effect of AQ on the conformation changes of HSA, UV–vis absorption spectra and synchronous fluorescence measurements were performed. UV–vis absorption spectroscopy as a simple technique can be used to explore the structural changes of protein and to investigate protein–ligand complex formation [46]. The UV–vis absorption spectra of HSA and 1:1 AQ–HSA complex are shown in Fig. 5A. The influences of AQ were eliminated by using corresponding concentration of AQ as reference solution during the measurement. It was observed that the addition

Table 4
Binding constants of competitive experiments of the AQ–HSA system (T = 291 K).

Site market	10^{-4} K_a (M^{-1})	[a]R
Blank	13.80	0.998
Ibuprofen	11.36	0.995
Warfarin	7.31	0.999

[a] R is the linear correlated coefficient.

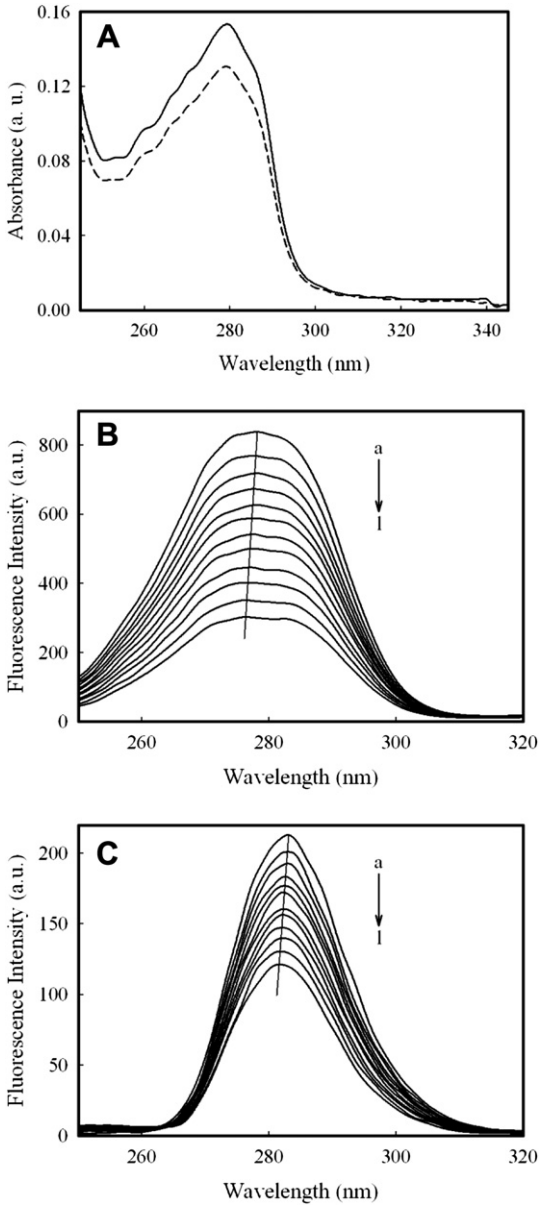

Fig. 5. (A) The UV–vis absorption spectra of HSA in the absence and presence AQ. Solid line, the absorption spectrum of HSA only and dash line, the absorption spectrum of HSA in the presence of AQ at the same concentration, $C_{HSA} = C_{AQ} = 4.0 \times 10^{-6}$ M; (B,C) The synchronous fluorescence spectra of HSA–AQ. (B) $\Delta\lambda$ = 60 nm; (C) $\Delta\lambda$ = 15 nm that $C_{HSA} = 1.1 \times 10^{-6}$ M while concentrations of AQ were from 0.0 to 15.0×10^{-6} M.

of AQ led to a small decrease in the HSA absorbance at 280 nm that could not be superposed within experimental error. As it is known, dynamic collision only affects the excitation state of quenching molecules, whereas it has no influence on the absorption spectra of quenching substances [21]. In contrast, ground state complex formation will frequently result in perturbation of the absorption spectrum of the fluorophore. Consequently a conclusion may be safely drawn that the probable fluorescence quenching mechanism of HSA by AQ is a static quenching procedure based on the formation of ground state complex between AQ and HSA. Meanwhile, the absorbance of HSA is characterized by a weak band at 280 nm that thought to be due to the aromatic amino acids (Trp, Tyr, and Phe). The decreased intensity of the peak at 280 nm indicate that the interaction between AQ and HSA leads to the loosening and unfolding of the protein skeleton while increasing the hydrophobicity of the microenvironment of the aromatic amino acid residues [47].

Synchronous fluorescence spectroscopy is a sensitive technique to analyze the micro-environmental changes of chromophores and have several advantages, including sensitivity, spectral simplification, and spectral bandwidth reduction and avoiding different perturbing effects [48]. The spectrum is obtained through the simultaneous scanning of excitation and emission monochromators of a fluorimeter, with a fixed wavelength difference ($\Delta\lambda$) between them. In the case of HSA, if $\Delta\lambda = 15$ nm, the synchronous fluorescence spectra exhibits the spectral character of the tyrosine residues alone, and if $\Delta\lambda = 60$ nm, it exhibits that of the tryptophan residues alone [42]. The effect of AQ on synchronous fluorescence spectra of HSA at $\Delta\lambda = 60$ and 15 nm are shown in Fig. 5B and C. Obviously, the quenching of the fluorescence intensity of tryptophan residues is stronger than that of tyrosine residue, suggesting that tryptophan residues contribute greatly to the quenching of intrinsic fluorescence of HSA. Moreover, a slight blue shift in maximum emission wavelength of tryptophan and tyrosine residue was observed upon addition of AQ, indicating that the conformation of HSA is changed such that the polarity around tryptophan and tyrosine residues is decreased and they are placed in a less hydrophobic environment [48]. These results suggested that AQ induces a conformational change in HSA.

3.6. Energy transfer between AQ and HSA

The distance between the binding site and the fluorophore in the protein can be evaluated according to the Förster mechanism of non-radiation energy transfer. According to Förster's theory [49], if the emitted fluorescence from a donor could be absorbed by an acceptor, the energy may transfer from the donor to the acceptor. The energy transfer effect is related not only to the distance between acceptor and donor (r), but also to the critical energy transfer distance (R_0), based on Eq. (6) [21]:

$$E = 1 - \frac{F}{F_0} = \frac{R_0^6}{R_0^6 + r^6} \tag{6}$$

where r is the distance between the acceptor (A) and the donor (D), R_0 is the critical distance when the transfer efficiency is 50%, which can be calculated by [21]:

$$R_0^6 = 8.79 \times 10^{-25} K^2 n^{-4} \phi J \tag{7}$$

In Eq. (7), K^2 is the spatial orientation factor of the dipole, n is the refractive index of the medium, ϕ is the fluorescence quantum yield of the donor and J is the overlap integral of the fluorescence emission spectra of the donor and the absorption spectra of the acceptor (Fig. 6), which can be calculated by the equation [21]:

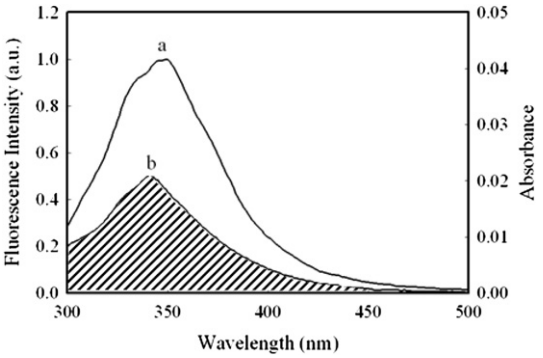

Fig. 6. The overlap of the fluorescence spectra (a) of HSA and the absorbance spectra (b) of AQ, $C_{HSA} = C_{AQ} = 1.1 \times 10^{-6}$ M (301 K).

$$J = \frac{\int_0^\infty F(\lambda)\varepsilon(\lambda)\lambda^4 d\lambda}{\int_0^\infty F(\lambda) d\lambda} \tag{8}$$

where $F(\lambda)$ is the fluorescence intensity of the fluorescent donor of wavelength λ, $\varepsilon(\lambda)$ is the molar absorption coefficient of the acceptor of wavelength λ. In the present case, $K^2 = 2/3$, $n = 1.336$, and $\phi = 0.118$ [50]. Hence, from Eqs. (6)–(8), we were able to calculate the following parameters, $J = 2.09 \times 10^{-14}$ cm^3 L mol^{-1}, $R_0 = 2.68$ nm, $E = 0.038$, and $r = 4.59$ nm. The donor to acceptor distance is less than 8 nm and $0.5R_0 < r < 2.0R_0$, which indicate that the energy transfer from HSA to AQ occurs with high probability [51].

3.7. Molecular docking studies

In this study, the Arguslab program was used to realize the binding mode of AQ at the active site of HSA. The main aspect for the ligand docking postures was considering the effective interaction of the drug with the various amino acid residues in the active site. The applied box size was 60 × 60 × 60 Å and grid resolution was 0.4 Å. Docking simulations were performed by selecting ArgusDock as the docking engine flexible for the drug. Finally the AScore was used as the scoring function. The binding site were obtained as Tyr150, Glu153, Ser192, Lys195, Gln196, Lys199, Trp214, Leu219, Phe223, Leu234, Leu238, His242, Arg257, Ile264, Ile290, Ala291 and Glu292. The binding constant and free energy change ΔG^0 for the binding of AQ to HSA were 1.43×10^5 M^{-1} and -29.58 kJ M^{-1}, respectively. These results are very close to those obtained by the above mentioned experimental method (Table 2).

The docking results showed that AQ binds within the binding pocket of sub-domain IIA (see Fig. 7A). The binding site of the HSA was studied to understand the nature of the residues defining the site. The distance between the AQ and the Trp214 was 4.6 Å that explain the fluorescence quenching of HSA emission in the presence of AQ. LIGPLOT was used to explore the hydrogen bonds interactions between HSA and AQ as shown in Fig. 7B. A hydrogen bonding interaction is observed between the hydroxyl (OH) group of AQ and Gln196 of HSA, with a distance of 2.23 Å.

3.8. Analysis of the dynamics trajectories

MD simulations were performed on HSA and HSA–AQ to investigate the dynamics properties of protein and complex in water by means of root mean square deviations (rmsd's) of protein

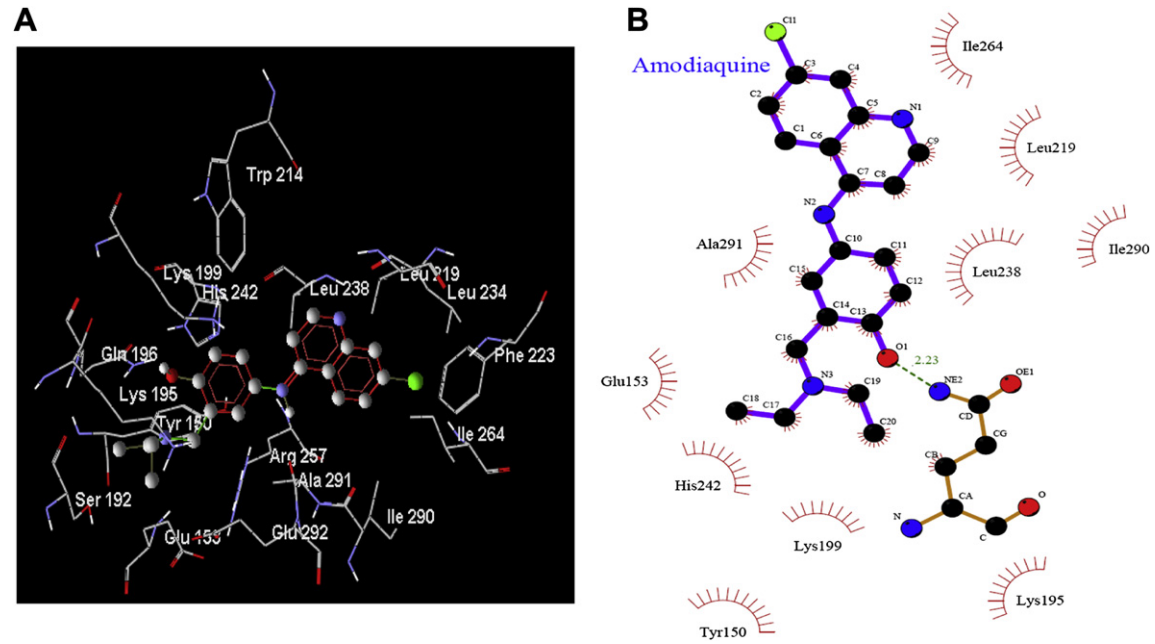

Fig. 7. (A) AQ docked in the binding pocket of HSA. AQ, depicted in a stick model (light green), and HSA, represented in solid (better) with a ray model; (B) Two-dimensional schematic representation of hydrogen bond interaction. Hydrogen bond depicted in dashed line. The figure was plotted using the program LIGPLOT (For interpretation of the references to color in this figure legend, the reader is referred to the web version of this article.).

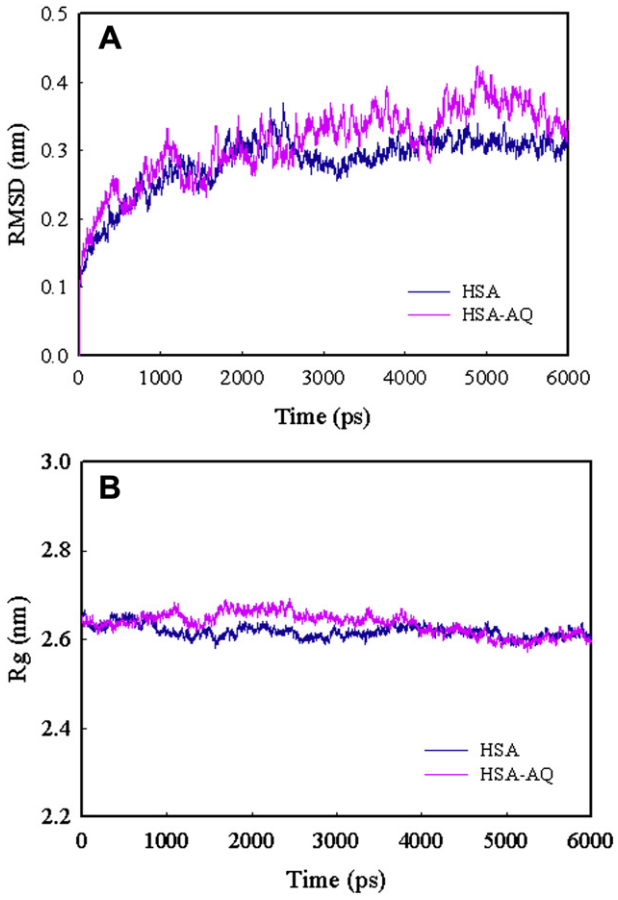

Fig. 8. (A) Time dependence of rmsd's. rmsd values for HSA and HSA–AQ complex during 6000 ps MD simulation; (B) Time evolution of the radius of gyration (Rg) during 6000 ps of MD simulation of HSA and AQ.

and complex with respect to the initial structure and the radius of gyration (Rg) of protein. The rmsd values of atoms in unliganded HSA and HSA–AQ complexes were plotted from 0 to 6000 ps as shown in Fig. 8A. Analysis of the Fig. 8A indicated that the rmsd of both systems reaches equilibration and oscillates around an average value after 3000 ps simulation time. The rmsd values of atoms in HSA and HSA–AQ complexes were calculated from a 3000–6000 ps trajectory, where the data points were fluctuated for HSA (0.303 ± 0.015 nm) and HSA–AQ (0.351 ± 0.026 nm). Moreover, radius of gyration (Rg) of protein and drug–protein complex is a measure of its compactness. Then, we determined the Rg values of HSA and HSA–AQ complex as shown in Fig. 8B. In both systems, Rg values were stabilized at about 3000 ps, indicating that the MD simulation achieved equilibrium after 3000 ps. Initially, the Rg values of both HSA and HSA–AQ complex was 2.65 nm. The HSA and HSA–AQ complex were stabilized at 2.615 ± 0.012 and 2.619 ± 0.020 nm, respectively. These results clearly indicate that the radius of gyration value is compatible upon AQ complexation with respect to free HSA. Therefore, it was concluded that the structure of the HSA in the presence of AQ stably folded during MD simulation.

4. Conclusions

This paper demonstrates a detailed investigation on the interaction between HSA and AQ using fluorescence techniques. The experimental data showed that the AQ could insert into the HSA and quench its intrinsic fluorescence by static mechanism, which was induced by the formation of the AQ–HSA complex because the Stern–Volmer quenching constant K_{sv} was inversely correlated with temperature. The apparent binding constants (K_a) between AQ and HSA were determined to be 1.38×10^5 (291 K), 8.39×10^4 (301 K) and $4.59 \times 10^4\ M^{-1}$ (310 K). The number of binding sites (n) for AQ was found to be about 1. By means of spectroscopy and molecular dynamic simulations, we have discovered and interpreted the alteration of the secondary structure of HSA by AQ complexation. The results of synchronous fluorescence spectroscopy indicated that

the polarity around tryptophan residues was increased whereas hydrophobicity around tyrosine residues was increased when AQ interacted with HSA, showing a slight change in the conformation of HSA upon addition of AQ under experimental conditions. According to the Förster theory of non-radiation energy transfer, the binding distances (r) between AQ and the tryptophan residue of HSA were calculated as 4.59 nm (301 K). The thermodynamic parameters $\Delta G^0 < 0$, $\Delta H^0 < 0$, and $\Delta S^0 < 0$ at different temperatures indicated that the binding process was spontaneous and hydrogen bonding interactions and Van der Waals force played the major role during the interaction between AQ and HSA. The independent molecular modeling studies resulted in binding constant and binding mechanism very close to the experimental ones. Both experimental and theoretical studies proposed that AQ binds to the sub-domain IIA or site I of HSA. This study is expected to provide important insight into the interactions of the physiologically important protein HSA with drugs and it is also looking forward for a further supplement and perfection.

Acknowledgment

Financial support of this project by Shiraz University Research Council is appreciated.

Appendix A. Supplementary material

Supplementary material associated with this article can be found, in the online version, at doi:10.1016/j.ejmech.2012.05.007.

References

[1] World Health Organisation, World Malaria Report 2010 (2010) Available at: http://www.who.int/malaria/publications/atoz/9789241564106/en/index.html (accessed on 25.04.12).
[2] S. Guglielmo, M. Bertinaria, B. Rolando, M. Crosetti, R. Fruttero, V. Yardley, S.L. Croft, A. Gasco, Eur. J. Med. Chem. 44 (2009) 5071–5079.
[3] http://en.wikipedia.org/wiki/Amodiaquine (accessed on 25.04.12).
[4] World Health Organisation, Global Report on Antimalarial Drug Efficacy and Drug Resistance: 2000–2010 (2010) pp. 30.
[5] X.M. He, D.C. Carter, Nature 358 (1992) 209–215.
[6] B. Sudhamalla, M. Gokara, N. Ahalawat, D.G. Amooru, R. Subramanyam, J. Phys. Chem. B 114 (2010) 9054–9062.
[7] Y. Zhang, B. Zhou, Y. Liu, C.X. Zhou, X.L. Ding, Y. Liu, J. Fluoresc 18 (2008) 109–118.
[8] B.P. Kamat, J. Seetharamappa, J. Pharm. Biomed. Anal. 35 (2004) 655–664.
[9] M.S. Dennis, M. Zhang, Y.G. Meng, M. Kadkhodayan, D. Kirchhofer, D. Combs, L.A. Damico, J. Biol. Chem. 277 (2002) 35035–35043.
[10] E. Froehlich, J.S. Mandeville, C.J. Jennings, R. Sedaghat-Herati, H.A. Tajmir-Riahi, J. Phys. Chem. B 113 (2009) 6986–6993.
[11] D. Charbonneau, M. Beauregard, H.A. Tajmir-Riahi, J. Phys. Chem. B 113 (2009) 1777–1784.
[12] P. Bourassa, I. Hasni, H.A. Tajmir-Riahi, Food Chem. 129 (2011) 1148–1155.
[13] J.S. Mandeville, E. Froehlich, H.A. Tajmir-Riahi, J. Pharm. Biomed. Anal. 49 (2009) 468–474.
[14] P. Bourassa, S. Dubeau, M.G. Maharvi, A.H. Fauq, T.J. Thomas, H.A. Tajmir-Riahi, Biochimie 93 (2011) 1089–1101.
[15] A. Belatik, S. Hotchandani, J. Bariyanga, H.A. Tajmir-Riahi, Eur. J. Med. Chem. 48 (2012) 114–123.
[16] F.P. Nicoletti, B.D. Howes, M. Fittipaldi, G. Fanali, M. Fasano, P. Ascenzi, G. Smulevich, J. Am. Chem. Soc. 130 (2008) 11677–11688.
[17] H.A. Tajmir-Riahi, J. Iran Chem. Soc. 3 (2006) 297–304.
[18] Y.V. Il'ichev, J.L. Perry, J.D. Simon, J. Phys. Chem. B 106 (2002) 452–459.
[19] F. Zsila, J. Visy, G. Mády, I. Fitos, Bioorg. Med. Chem. 16 (2008) 3759–3772.
[20] B. Birdsall, R.W. King, M.R. Wheeler, C.A. Lewis, S.R. Goode, R.B. Dunlap, G.C.K. Roberts, Anal. Biochem. 132 (1983) 353–361.
[21] J.R. Lakowicz, Principles of Fluorescence Spectroscopy, third ed. Springer Science+Business Media, New York, 2006.
[22] ArgusLab 4.0.1, Mark A. Thompson Planaria Software LLC, Seattle, WA http://www.arguslab.com (accessed on 25.04.12).
[23] A.C. Wallace, R.A. Laskowski, J.M. Thornton, Protein Eng. 8 (1995) 127–134.
[24] R. Vandrunen, Comput. Phys. Commun. 91 (1995) 43–56.
[25] E. Lindahl, B. Hess, J. Mol. Model. 7 (2001) 306–317.
[26] I.G. Tironi, Biomolecular Simulation: The GROMOS 96 Manual and User Guide (1996) Switzerland.
[27] U. Essmann, L. Perera, M.L. Berkowitz, T. Darden, H. Lee, L.G. Pedersen, J. Chem. Phys. 103 (1995) 8577–8593.
[28] W.C. Swope, H.C. Andersen, P.H. Berens, K.R. Wilson, J. Chem. Phys. 76 (1982) 637–649.
[29] E.H. Kennard, Kinetic Theory of Gases, McGraw-Hill, New York, 1963.
[30] A.W. Schuttelkopf, D.M.F.V. Aalten, Acta Crystallogr. 60 (2004) 1355–1363.
[31] H.J.C. Berendsen, J.R. Grigera, T.P. Straatsma, J. Phys. Chem. 91 (1987) 6269–6271.
[32] H.C. Andersen, J. Chem. Phys. 72 (1980) 2384–2393.
[33] H.J.C. Berendsen, J.P.M. Postma, W.F.V. Gunsteren, A. Dinola, J.R. Haak, J. Chem. Phys. 81 (1984) 3684–3690.
[34] J.R. Lakowicz, G. Weber, Biochemistry 12 (1973) 4161–4170.
[35] Y.-J. Hu, Y. Liu, X.-H. Xiao, Biomacromolecules 10 (2009) 517–521.
[36] Y. Hu, Y. Liu, J. Wang, X. Xiao, S. Qu, J. Pharm. Biomed. Anal. 36 (2004) 915–919.
[37] I.M. Klotz, Ann. N. Y. Acad. Sci. 226 (1993) 18–35.
[38] P.D. Ross, S. Subramanian, Biochemistry 20 (1981) 3096–3102.
[39] T.C. Pinkerton, K.A. Koeplinger, Anal. Chem. 62 (1990) 2114–2122.
[40] B. Ojha, G. Das, J. Phys. Chem. B 114 (2010) 3979–3986.
[41] J. Rohacova, M.L. Marin, M.A. Miranda, J. Phys. Chem. B 114 (2010) 4710–4716.
[42] N. Ibrahim, H. Ibrahim, S. Kim, J.-P. Nallet, F. Nepveu, Biomacromolecules 11 (2010) 3341–3351.
[43] X. Qu, T. Komatsu, T. Sato, O. Glatter, H. Horinouchi, K. Kobayashi, E. Tsuchida, Bioconjug. Chem. 19 (2008) 1556–1560.
[44] F. Samari, B. Hemmateenejad, M. Shamsipur, M. Rashidi, H. Samouei, Inorg. Chem. 51 (2012) 3454–3464.
[45] B.C.G. Karlsson, A.M. Rosengren, P.O. Andersson, I. Nicholls, J. Phys. Chem. B 111 (2007) 10520–10528.
[46] Z. Chi, R. Liu, Y. Teng, X. Fang, C. Gao, J. Agric. Food Chem. 58 (2010) 10262–10269.
[47] Z. Chi, R. Liu, Biomacromolecules 12 (2011) 203–209.
[48] Y.-J. Hu, Y. Liu, Z.-B. Pi, S.-S. Qu, Bioorg. Med. Chem. 13 (2005) 6609–6614.
[49] T. Förster, Ann. Phys. 2 (1948) 55–75.
[50] F.-L. Cui, J. Fan, J.-P. Li, Z.-D. Hu, Bioorg. Med. Chem. 12 (2004) 151–157.
[51] B. Valeur, Molecular Fluorescence: Principles and Applications, Wiley, New York, 2001.